ELSEVIER

Journal of Chromatography A, 910 (2001) 127–135

JOURNAL OF CHROMATOGRAPHY A

www.elsevier.com/locate/chroma

On-line packed column supercritical fluid chromatography–microwave-induced plasma atomic emission

Fabrice Bertoncini[a], Didier Thiébaut[a,*], Marcel Caude[a], Mathias Gagean[b], Bernadette Carrazé[c], Pascal Beurdouche[d], Xavier Duteurtre[d]

[a]*Laboratoire Environnement et Chimie Analytique (associated to CNRS), Ecole Supérieure de Physique et de Chimie Industrielles de Paris, 10 Rue Vauquelin, 75231 Paris Cedex 05, France*

[b]*PSA Peugeot–Citroën, 25420 Voujeaucourt, France*

[c]*PSA Peugeot–Citroën, Route de Gisy, 78140 Velizy-Villacoublay, France*

[d]*Renault S.A. Technocentre, 78288 Guyancourt Cedex, France*

Received 12 April 2000; received in revised form 26 October 2000; accepted 7 November 2000

Abstract

Interfacing and evaluation of packed column supercritical fluid chromatography (SFC)–microwave-induced plasma atomic emission detection (AED) is described. Via a flow splitter and an integral restrictor, efficient transfer of solutes from column to detector without band broadening is obtained. Variation of CO_2 flow-rate during pressure gradients has little influence on both AED signal and baseline drift while it provides similar sensitivity as in capillary SFC. Continuous introduction of CO_2 in the plasma reduces the available range of emission domains; nevertheless the region of detection which is free of CO_2 interferences allows selective detection of Cl and Br as reported in this paper.

Keywords: Atomic emission detection; Microwave-induced plasma; Detection, SFC; Phenylureas

1. Introduction

The potential of supercritical fluid chromatography (SFC) has been demonstrated by analyzing compounds not easily amenable to gas chromatography (GC) owing to their poor thermal stability or volatility and by better kinetics and detection features than liquid chromatography (LC). Most of the LC and GC detectors have been hyphenated to SFC. However, for multi-element simultaneous detection, hyphenation of many of these detectors is required.

In the course of developing a multi-element specific detector for SFC, attempts have been made to implement atomic emission detection (AED) which selectivity and sensitivity features make the SFC–AED on-line coupling very attractive for analytical purpose.

Inductively coupled plasma (ICP) [1–7] and microwave-induced plasma (MIP) have been used for atomization in AED and coupled with chromatographic systems.

MIP-AED coupling with SFC was investigated because, after McCormack et al.'s [8] pioneering

*Corresponding author. Tel.: +33-1-4079-4648; fax: +33-1-4079-4776.

E-mail address: didier.thiebaut@espci.fr (D. Thiébaut).

0021-9673/01/$ – see front matter
PII: S0021-9673(00)01121-3

work in 1975 and the introduction of the TM_{010} type microwave cavity by Beenakker [9], GC–AED has gained a real interest in analytical fields for detection of halogens in pesticides [10], speciation [11], analysis of organic pollutants [12] or as a complement to mass spectrometry data for identification purposes [13]. As SFC detectors, laboratory-made microwave torch plasma (MPT) [14], radio frequency plasma (RFD) [15], and the two most widespread ones, TM_{010} Beenakker cavity [16] and surface wave sustained plasma (or surfatron), were evaluated [17–20]. As the surfatron is hardly compatible with high CO_2 flow-rate, the modified Beenakker resonant cavity was preferred for both capillary and packed column SFC [21–23] using helium plasma over argon for the detection of metals and non-metals [24]. A moderate power plasma was more stable with supercritical effluent of micro-packed columns [25,26] and MIP-AED was also implemented with binary mobile phase [27].

This paper reports the first results on the hyphenation of conventional packed column SFC to an MIP-AED system designed for GC coupling; conditions of interfacing SFC to MIP-AED, capabilities and limitations of the technique are discussed.

2. Experimental

The SFC–MIP-UV system used for this study is described below and shown in Fig. 1.

2.1. Supercritical fluid chromatograph

A Hewlett-Packard G 1205 A supercritical fluid chromatograph equipped with a flame ionization detection (FID) system and a HP 1050 multiwavelength photodiode array detection (DAD) system was used. Column outlet pressure was controlled with the backpressure regulator and injections were made using a Rheodyne Model 7413 valve with a 5-μl loop. The injector was air actuated to enable a 4-s injection. The integral restrictor was made in the laboratory from a 50 μm I.D. deactivated fused-silica capillary tubing from S.G.E. (Villeneuve St.

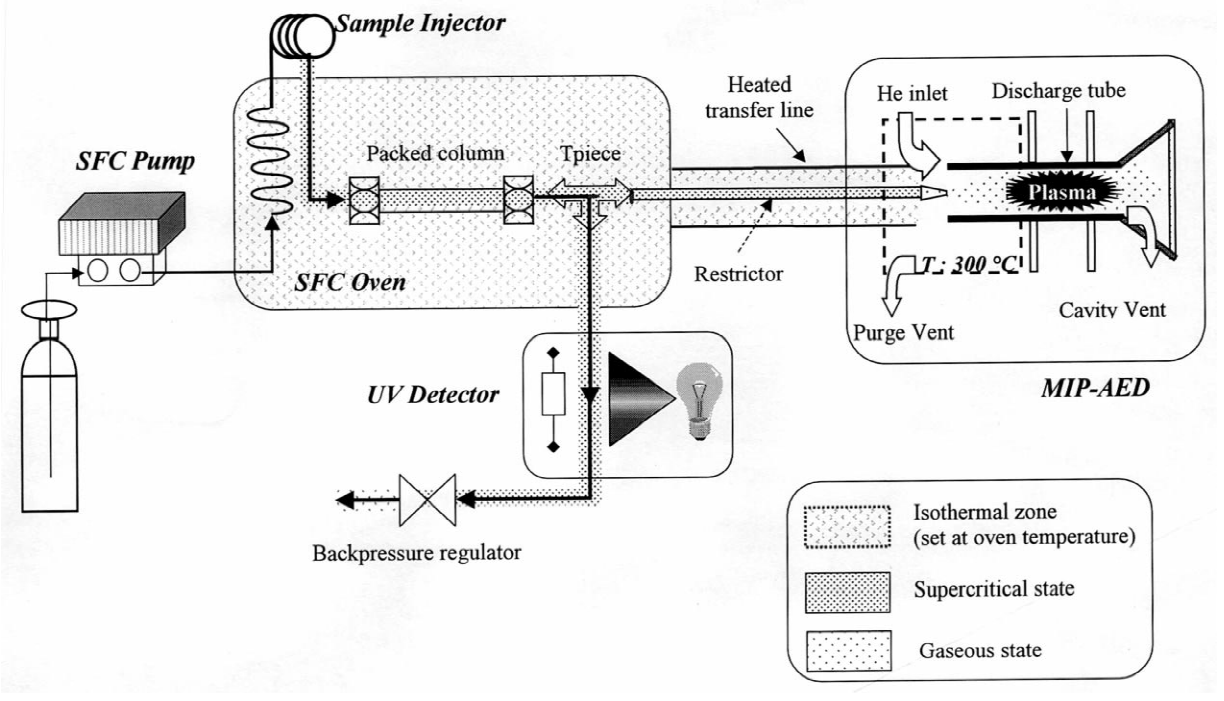

Fig. 1. Schematic diagram of the on-line SFC–MIP-AED–UV assembly.

Georges, France). The mobile phase was SFC-grade carbon dioxide from Air Liquide (Nanterre, France).

Two packed columns were used: a Gammabond RP-18 250×4.6 mm, 5 μm and a Capcell Pak C_{18} 250×4.6 mm, 5 μm both from Interchim (Montluçon, France).

Research-grade chlorobenzene and 1-bromoanthracene were obtained from Aldrich (Lyon, France) and phenylurea pesticides were obtained from CIL (Sainte-Foy-la-Grande, France).

2.2. Microwave-induced plasma atomic emission detector

The GC–AED set up consisted of a HP G 2350 A atomic emission detector coupled to a HP 6890 gas chromatograph (Agilent Technologies, Les Ulis, France). AED reagent gases and He plasma make up were piloted by the electronic pneumatic controller module of the GC system. Helium (N 60), Ar (N 56), H_2 (N 55) and O_2 (N 55) were purchased from Air Liquide. The plasma was sustained inside a 4.25 mm×1 mm I.D.×1.25 mm O.D. quartz tube.

The optical assembly and the spectrometer were purged by argon at flow-rate of 2 l/min.

Other chromatographic conditions are listed in Table 1.

Spectral data are collected on a 25-nm wide wavelength region containing the emission lines of the element(s) of interest. Other emission lines can only be used for acquisition if they are within 25 nm of the emission lines selected by the manufacturer. The current emission line is fine-tuned automatically including background treatment.

In GC, the column effluent introduced into the plasma commonly has a flow-rate of about 2 ml/min and the helium flow-rate is typically set at 35 ml/min.

Table 1
Chromatographic conditions

AED		
Temperature	Cavity	300°C
	Transfer line	80°C
Gases set up	Cavity pressure	1.5 p.s.i.[a]
	Purge vent	50 ml/min
	Cavity vent	55–155 ml/min
	He make up gas flow-rate	20–130 ml/min
	Regent gas pressure O_2	26 p.s.i.
Data rate		5 Hz
SFC	Oven temperature	80°C
	Injection loop	5 ml
	Column flow-rate	2 ml/min
	Pressure	100–300 atm[b]
	Ramping rate	20 atm/min
	Split ratio	0.007–0.02

[a] 1 p.s.i.=6894.76 Pa.
[b] 1 atm=101 325 Pa.

2.3. SFC–MIP interface

Fig. 1 shows a diagram of the SFC–MIP-AED interface. The flow-rate of the mobile phase was split so only ca. 1% of the column effluent reached the AED system via an integral fused-silica restrictor connected to a T-piece. Instead of the GC column, the integral restrictor was introduced into the transfer line between the GC oven and the MIP-AED system so the restrictor outlet was in the discharge tube; the 1 mm I.D. stainless steel tubing used for GC column introduction into the transfer line was used without modification. The transfer line can be heated from ca. 90°C (depending on both the cavity and the oven temperature) to 450°C. The temperature of the cavity block was set at 350°C; for SFC purposes, it must be high enough to compensate for the Joule–Thompson cooling effect occurring when the CO_2 is decompressed. The CO_2 expanded flow-rate from the restrictor was 7 ml/min at 100 atm under the conditions shown in Table 1 (1 atm=101 325 Pa).

3. Results and discussion

3.1. Initial conditions for lightening the plasma

Conditions were chosen so the CO_2 expanded flow from the restrictor was kept as similar as possible to the conventional GC capillary column flow-rate, ca. several ml/min using laboratory-made integral restrictors (7 ml/min at 100 atm and 300°C). Using splitting of column effluent, conventional packed columns could be used while a low flow-rate was introduced into the MIP-AED system (Fig. 1); thus, independent control of pressure and column flow-rate was possible because the CO_2 flow-rate at the UV detector outlet was high enough to ensure reliable

pressure control using the automatic pressure regulator of the apparatus in the so called ''downstream'' mode.

Owing to the complex flow scheme of the gases involved in MIP-AED, it was necessary to check the whole CO_2 flow-rate at the restrictor outlet was entering the discharge tube and reaching the He plasma: both purge vent and cavity vent flow-rates (Fig. 1) were monitored before lightening the plasma. When the CO_2 was added, the former was unchanged whereas the latter increased cavity vent and restrictor flow-rates, indicating that the mobile phase introduced in the discharge tube was not split to the purge vent before reaching the plasma.

Under these conditions, the plasma was easily lightened. No thermally degradation of the tip of the restrictor was observed indicating it was far enough from the plasma.

Because CO_2 was introduced continuously into the plasma, the plasma became green (C_2 emission line at 512 nm [17], proving the mobile phase swept through the plasma was atomized) instead of pink and its size seemed to constrict. The decrease of ionized gas volume may indicate there is only partial excitation of the mobile phase molecules. To avoid carbon deposition [28], a small amount of O_2 acting as a scavenger was added to the plasmagen gas. Stability of the plasma was obtained for a He flow-rate higher than 35 ml/min. The effect of both helium and the CO_2 flow-rates on the plasma will be discussed further in this paper.

3.2. Effect of introduction of CO_2 on the spectral data

As a result of mobile phase decomposition, specific emissions of ionic and molecular lines of CO and molecular lines of C_2 and CN were observed. The latter indicates nitrogen (from air?) was present in the plasma and was eliminated by efficient argon purging of the transfer line and the plasma cavity giving rise to great expectations for nitrogen detection at 388 nm using our system. The others produce numerous emission lines so part of the spectral range becomes obscure and the range 180–220 nm is not available for data acquisition (cf. Ref. [18]). Nevertheless, detection of hydrogen (486 nm), boron (250 nm), iron (302 nm), fluorine (690 nm), tin (271 and 326 nm), bromine (479 and 827 nm), and chlorine (478 and 837 nm) is possible. Elements having intense emission lines in the 180–200 nm domain such as phosphorus (186 nm), sulfur (181 nm), nitrogen (174 nm) or selenium (184 nm) could be detected using alternative emission wavelengths which require software modification.

As a result, chlorinated and brominated molecules (phenylureas and chlorobenzene) were selected as test compounds for evaluation of the capabilities of SFC–MIP-AED hyphenation.

A comparison of signal intensity for the ionic and atomic emission lines of Cl at 479 and 837 nm, respectively, was performed. Results are shown in Fig. 2. Compared to the signal measured at 479 nm, the signal intensity measured at 837 nm is 16 times higher. Explanations rely on: (i) the lack of interference in the near IR region compared to UV–Vis region where Cl(II) ionic emission line is overlapped by the C_2 emission band region (450–560 nm

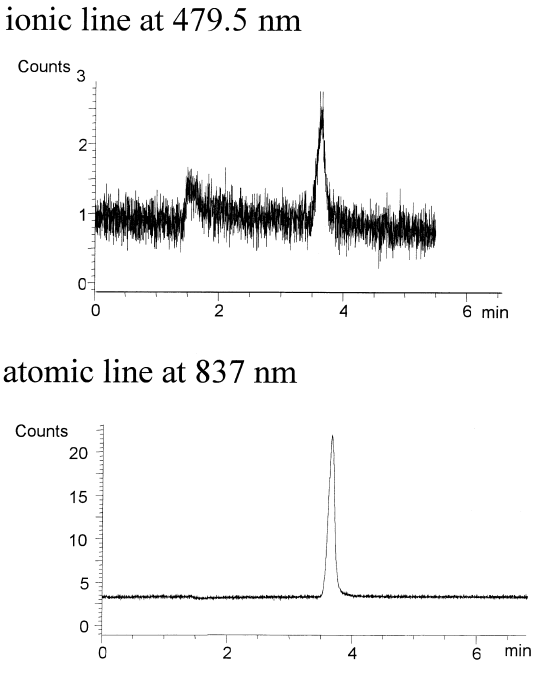

Fig. 2. Comparison of Cl atomic and ionic emission lines intensity from replicate injection of 1.05 mg of chlorobenzene. AED conditions: He flow-rate, 35 ml/min; O_2 pressure, 26 p.s.i. Column ''Gammabond RP C_{18}'' 250×4.6 mm, 5 μm; column pressure, 100 atm; CO_2 density, 0.23 g/ml, other conditions as in Table 1.

approximately); (ii) the emission from the chlorine ion at 479 nm is based upon charge transfer between ground state ionized helium and ionized excited chlorine [29,30] and could only occur in helium plasma discharge [31]; the presence of CO_2 in the plasma could destabilize the charge transfer process; (iii) possible quenching of chlorine ionic radiation by the CO_2 doped plasma.

Thus, 827 and 837 nm were selected, respectively, for Br and Cl emission line acquisition.

3.3. Effect of CO_2 flow-rate on chlorine emission intensity

The quantity of CO_2 introduced into the plasma per unit of time depends on the volumetric flow-rate delivered by the restrictor as a function of pressure and temperature. For a given restrictor, increasing the pressure of the mobile phase increases the CO_2 flow-rate in the plasma. The effect of the variation of the amount of CO_2 introduced in the plasma was studied by monitoring the Cl signal intensity (peak area) for successive injections of the same injected quantity of chlorobenzene at different pressures. As the CO_2 pressure was increased in the column, the split ratio varied from 0.7 to 2% indicating that a higher amount of CO_2 (and chlorobenzene) was entering the AED system. Results are shown in Fig. 3: signal intensity decreased as CO_2 pressure was increased despite an increase of amount of chlorobenzene reaching the plasma owing to the change of split ratio; there is a slight decrease of response in the range from 140 to 180 atm followed by a fast decrease as pressure/CO_2 flow-rate was further increased. These results are quite different from those obtained in capillary SFC–MIP [21,22] and low powered packed column SFC–MIP [26] where a linear and continuous decrease of Cl signal intensity was observed. This behavior is probably related to the higher range of flow-rates investigated and to the split ratio variation during the experiments compared to previous data: the increase of amount of solute reaching the plasma partially compensates for the decrease of signal occurring when the CO_2 flow-rate increases (first part of the curve).

A very important point is that the plasma was not blown during these experiments indicating the detector could be used during pressure gradients despite a reduction of signal intensity.

Thus, the behavior of the detector was studied in pressure gradient mode: the CO_2 pressure was initially set at 100 atm and ramped to 300 atm at 20 atm/min. Cl emission signals at 837 nm obtained under isobaric conditions and using the pressure gradient were compared: a low baseline drift occurs in the trace corresponding to pressure ramping conditions. However, it does not preclude quantitative analysis via AED acquisition and looks much less important than drifts reported using capillary SFC–Surfatron [18–20] and capillary SFC–low po-

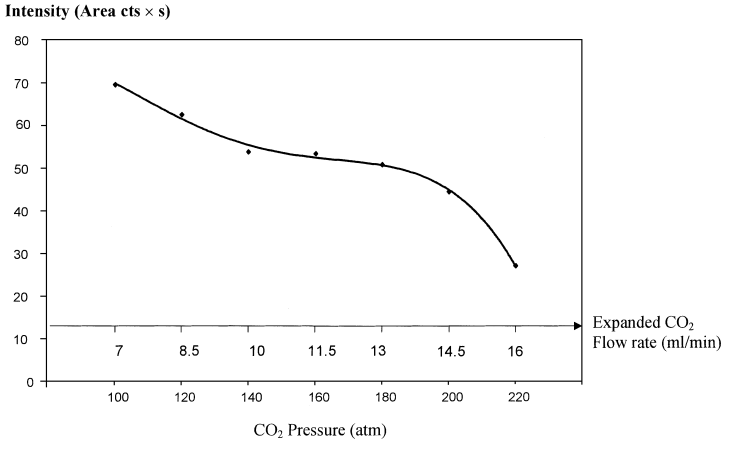

Fig. 3. Effect of CO_2 flow-rate on 837 nm Cl emission line intensity from replicate injections of chlorobenzene. Same conditions as in Fig. 2, except the SFC pressure which was incremented for each experiment.

wered MIP [21]. This confirms the good tolerance of this detector for changes of CO_2 flow-rates. Comparison of peak area shows only a 10% signal intensity depression in pressure ramping conditions compare to isobaric conditions. Using the pressure program, chlorobenzene elutes earlier and for a higher CO_2 flow-rate in the restrictor (11.5 ml/min) than under isobaric conditions; subsequently, the AED signal must be lower according to the data presented in Fig. 3. However, there is, as described above, partial compensation of signal decrease at 160 bar compared to 100 bar as the amount of chlorobenzene reaching the plasma is higher at 160 bar than at 100 bar owing to the split ratio variation versus pressure.

3.4. Effect of helium flow-rate on Cl signal intensity

The effect of helium flow-rate on emission intensity was studied using constant chromatographic conditions and chlorobenzene as a test compound with the aim to compensate for the signal depletion occurring when the amount of CO_2 introduced in the plasma increases.

Fig. 4 shows the peak area of chlorobenzene versus He flow-rate: the signal increases until a plateau is reached above 80 ml/min. Standard deviation reported in Fig. 4 is much higher at low flow-rates and can be explained by plasma instability. Indeed, the appearance of plasma was changing in the course of experiment: it had a greenish color at high flow-rate turning to pink at very low He flow (less than 25 ml/min). As the greenish color is caused by the C_2 emission band (at 512 nm), He flow-rates higher than 30 ml/min are required for efficient ionization of CO_2 and excitation of analytes; further, a better stabilization of emission signal is also obtained.

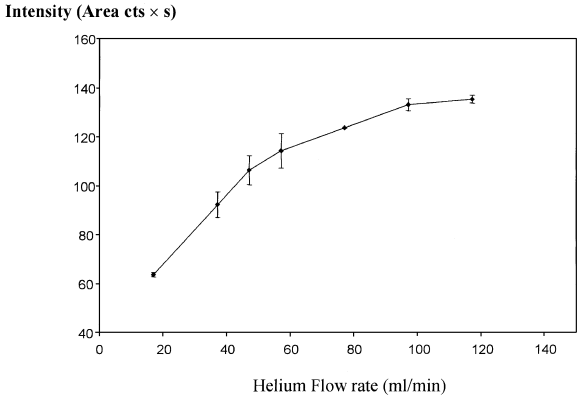

Fig. 4. Effect of He flow-rate on 837 nm Cl emission line from replicate injections of chlorobenzene. Same conditions as in Fig. 2.

At high flow-rates, the change in behavior could be the consequence of antagonist effects between improving the efficiency of the plasma by increasing the amount of plasmagen gas and decreasing atomization efficiency owing to the decrease of the residence time in the plasma consecutive to the increase of linear velocity in the discharge tube [27]. As a result, further increase of the helium flow-rate could lead to a decrease of the response indicating a maximum could be reached for achieving the best detection conditions to advantage for sensitivity.

It is worth noting that the transfer line designed for the GC coupling of the MIP-AED system and a flow splitter placed in the GC oven at column outlet were suited for SFC coupling: the reduced plate heights for chlorobenzene in the UV and MIP-AED traces were 3.2 and 2.9, respectively. The 10% loss of theoretical plates reported for UV detection came from the long connection tubing (ca. 1 m) between the T-piece and the UV detector flow cell owing to system arrangement favoring interfacing of SFC to the AED system rather than to the UV detector.

3.5. Application to the detection of phenylurea herbicides

Four phenylureas whose log *P* ranges from 2.30 to 3.09 were selected as test compounds. They were separated with neat CO_2 as the mobile phase using a Capcell Pak C_{18} column and a pressure gradient (Fig. 5). UV and halogen AED traces showing similar efficiencies were obtained. However, compared to UV, noise is evident on the AED trace and detection of compounds required high sample concentration, ca. 0.02 mol/l; detection limits are gathered in Table 2 and can be compared to chlorine, bromine and hydrogen detection limits reported in the literature with SFC–MIP systems. The values reported in Table 2 are quite similar to those obtained using moderate power SFC–MIP systems

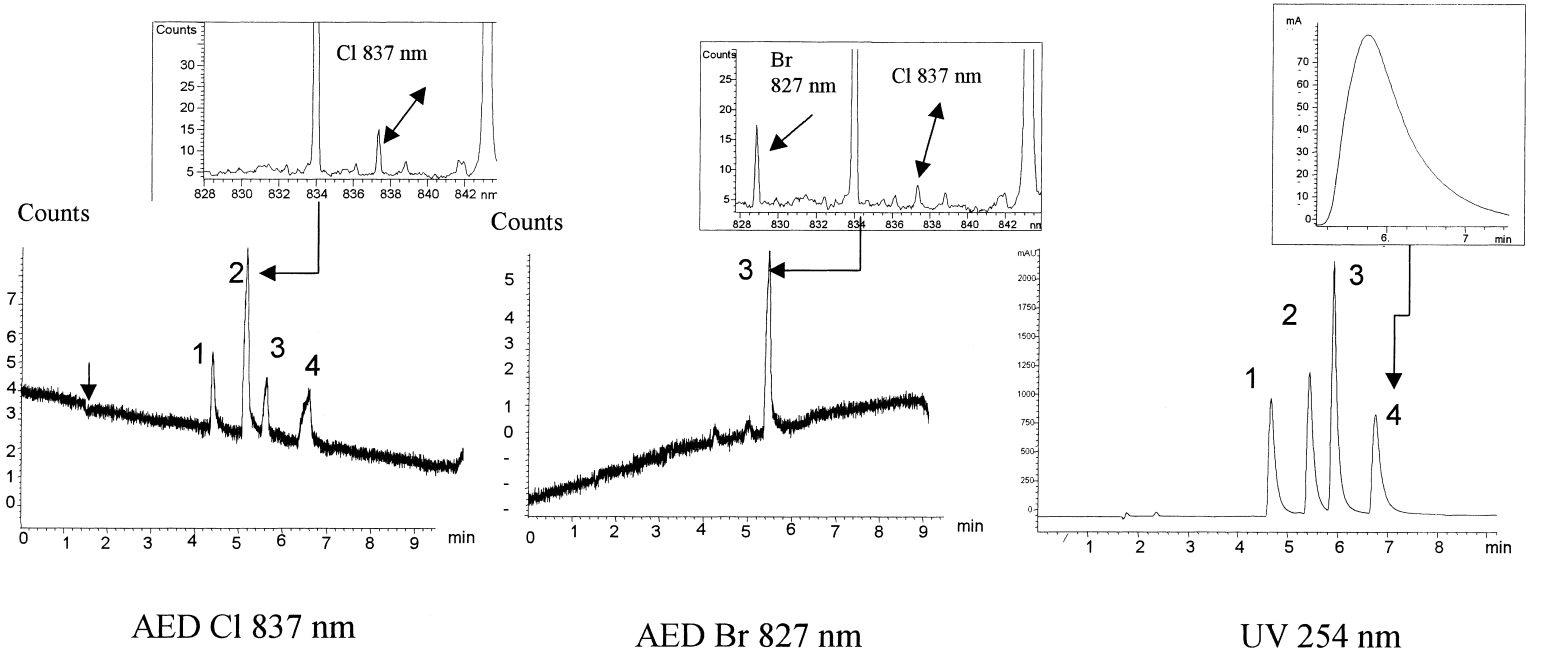

Fig. 5. AED and UV traces of the separation of a phenylureas mixture with neat CO_2. AED conditions: He flow-rate, 120 ml/min; O_2 pressure, 26 p.s.i. Column ‘‘Capcell Pack C_{18}’’ 250×4.6 mm; pressure programming; initial pressure, 100 atm; final pressure 300 atm; pressure ramp, 20 atm/min; oven temperature: 80°C; column flow-rate: 2 ml/min (5°C). Solutes: 1=monolinuron; 2=linuron; 3=chlorbromuron; 4=diuron.

Table 2
Detection limit for the SFC–MIP-AED system using CO_2 as mobile phase

Element	Wavelength (nm)	LOD (ng/s)	Cavity design	Column	Ref.
Cl	837.8	1.7	TM_{010} (60 W)	Packed	This work[a]
	837.8	1.5	TM_{010} (500 W)	Packed	[26]
	837.8	ca. 2.5	TM_{010}	Packed	[22]
	837.8	0.04	TM_{010}	Capillary	[21]
	837.8	0.21	Surfatron	Capillary	[18]
Br	827.2	0.76	TM_{010} (60 W)	Packed	This work[a]
		0.78	Surfatron	Capillary	[18]

[a] This work, same conditions as in Fig. 2 except column pressure, 200 bar.

[26] and better than previous work using a packed column [22]. These first results are quite promising as the detection limit level of bromine at 827 nm is very close to the value obtained by Luffer and Novotny [18] using capillary SFC–AED despite being, by far, too high for the sensitive analysis of halogen compounds under SFC conditions. For chlorine at 837 nm, the detector response versus the concentration was linear ($r^2=0.993$) from 0.1 to 50 μg (at 7 ml/min and 110 ml/min of CO_2 and He flow-rates, respectively).

In the AED trace, the elution peak of diuron exhibits front tailing; this effect is much less pronounced in the enlarged UV trace. Owing to the amount injected, bad solubility of the compound in the CO_2 during the injection is likely to occur leading to front tailing on the elution peak, partially explaining the bad peak shape observed in the AED trace; further to the injected quantity, explanations of this shape could also involve: (i) a bad transfer in the plasma by the interface owing to restrictor partial plugging or more likely temperature difference between the transfer line and the column oven because the temperature of the transfer line was 20°C higher than oven temperature or (ii) more complex effects in emission mechanisms as has been assessed above for pressure programmed separations.

Nevertheless, element and molecule specific information are provided allowing selective detection of phenylureas. After optimization, SFC–AED could be involved for their identification in complex environmental matrices where number of interferents reduce the potential of UV–DAD owing to the similarity of UV spectra of phenylureas.

3.5.1. Response factor

Two sets of triplicate injections of the mixture of phenylureas were carried out under isobaric and pressure ramping conditions. The molar response factor R was calculated and normalized to the average response factor of the phenylureas.

Under isobaric conditions, the response factors are close to 1 ($\sigma=7\%$) even though the concentration and the number of chlorine per molecule are different. Thus, MIP enables decomposition of phenylureas into free atoms so the emission yield is related to the elemental concentration in the plasma as reported in GC–AED [32,33].

Under pressure ramping conditions, as in capillary SFC–MIP [21], the standard deviation of the normalized response factors increases to 14% because there is a slight decrease of AED signal versus the CO_2 flow-rate leading to a decrease of R despite the split ratio increases.

4. Conclusion

Conventional packed column SFC can be hyphenated to a GC designed MIP-AED system with minor changes to the column–AED system interface design. With proper set up of operating conditions, it allows detection of many elements using the same treatment of signal as in GC. However, owing to the emission related to continuous CO_2 introduction into the plasma, for some major elements such as S, selection of alternative emission lines is required with software revision to enable powerful signal treatment. Yet, detection capabilities for Cl and Br

are close to the values previously reported with response factors close to unity. Compared to GC, detection limits are much higher and further optimization of the coupling is needed to improve both sensitivity and number of elements to be detected. The use of SFC–MIP for nitrogen and other element detection is being carried out with neat carbon dioxide as the mobile phase to advantage for better direct investigation of oil additives which can be eluted without polar modifiers [34]. Nevertheless, in order to broaden the application field of AED to higher polarity compounds such as pharmaceutical compounds, the effect of polar modifiers on AED capabilities will also be investigated.

Acknowledgements

The financial support of Renault S.A. and PSA Peugeot–Citroën for this work is deeply acknowledged. The authors are very grateful to M. Carroué from Agilent Technologies France for his help in starting with AED and coupling to SFC.

References

[1] J.W. Olesik, S.V. Olesik, Anal. Chem. 59 (1987) 796.
[2] C. Fujimoto, H. Yoshida, K. Jinno, J. Chromatogr. 411 (1987) 213.
[3] W.L. Shen, N.P. Vela, B.J. Sheppard, J.A. Caruso, Anal. Chem. 63 (1991) 1491.
[4] N.P. Vela, L.K. Olson, J.A. Caruso, Anal. Chem. 65 (1993) 585A.
[5] E. Blake, M.W. Raynor, D. Cornell, J. Chromatogr. A 683 (1994) 223.
[6] E. Blake, M.W. Raynor, D. Cornell, J. High Resolut. Chromatogr. 18 (1995) 33.
[7] S. Liang, D.C. Tilotta, Anal. Chem. 70 (1998) 4487.
[8] A.J. McCormack, S.C. Tong, W.D. Cooke, Anal. Chem. 37 (1965) 1470.
[9] C.I.M. Beenakker, Spectrochim. Acta 31B (1976) 483.
[10] S. Pedersen-Bjergaard, T. Greibrokk, J. High Resolut. Chromatogr. 19 (1996) 597.
[11] R. Lobinski, F.C. Adams, Trends Anal. Chem. 12 (1993) 41.
[12] H. Mol, T. Hankemeier, U.A.Th. Brinkman, LC–GC Int. 12 (1999) 108.
[13] H. Frischenschlager, C. Mittermayr, M. Peck, E. Rosenberg, M. Grasserbauer, Fresenius J. Anal. Chem. 359 (1997) 213.
[14] J. Qinhan, F. Wang, C. Zhu, D.M. Chambers, G.M. Hieftje, J. Anal. Atom. Spectrom. 5 (1990) 487.
[15] R.J. Skelton, P.B. Farnworth, K.E. Marksides, M.L. Lee, Anal. Chem. 61 (1989) 1815.
[16] G.L. Long, G.R. Ducatte, E.D. Lancaster, Spectrochim. Acta 49B (1994) 75.
[17] L.J. Galante, M. Selby, D.R. Luffer, G.M. Hieftje, M. Novotny, Anal. Chem. 60 (1988) 1370.
[18] D.R. Luffer, M. Novotny, J. Chromatogr. 517 (1990) 477.
[19] D.R. Luffer, M. Novotny, J. Microcol. Sep. 3 (1991) 39.
[20] D.R. Luffer, L.J. Galante, A.D. Paul, M. Novotny, G.M. Hieftje, Anal. Chem. 60 (1988) 1365.
[21] L. Zhang, J.W. Carnahan, R.E. Winans, P.H. Neil, Anal. Chem. 63 (1991) 212.
[22] C.B. Motley, G.L. Long, J. Anal. Atom. Spectrom. 5 (1990) 477.
[23] C.B. Motley, G.L. Long, Appl. Spectrosc. 44 (1990) 667.
[24] C.B. Motley, M. Ashraf Khorassani, G.L. Long, Appl. Spectrosc. 43 (1989) 737.
[25] G.K. Webster, J.W. Carnahan, Appl. Spectrosc. 45 (1991) 1285.
[26] G.K. Webster, J.W. Carnahan, Anal. Chem. 64 (1992) 50.
[27] Y. Wang, J.W. Carnahan, Anal. Chem. 65 (1993) 3290.
[28] A. De Wit, J. Beens, in: E.R. Adlard (Ed.), Chromatography in the Petroleum Industry, Elsevier, Amsterdam, 1995, Chapter 7.
[29] A. Goldwasser, J.M. Mermet, Spectrochim. Acta 41B (1986) 725.
[30] J.W. Carnahan, G.M. Hieftje, Spectrochim. Acta 47B (1992) 731.
[31] P.A. Brandl, J.W. Carnahan, Spectrochim. Acta 49B (1994) 105.
[32] P.C. Uden, K.J. Sleetkavitz, R.M. Barnes, R.L. Deming, Anal. Chim. Acta 180 (1986) 401.
[33] C. Webster, M. Cooke, J. High Resolut. Chromatogr. 18 (1995) 319.
[34] F. Bertoncini, D. Thiebaut, P. Valette, B. Carraze, Chromatographia, submitted for publication.